Scanning Microscopy

Volume 1992
Number 6 *Signal and Image Processing in Microscopy and Microanalysis*

Article 29

1992

Automatic Orientation Analysis of Microfabric

N. K. Tovey
University of East Anglia, United Kingdom

P. Smart
University of Glasgow, United Kingdom

M. W. Hounslow
University of East Anglia, United Kingdom

J. P. Desty
University of East Anglia, United Kingdom

Scanning Microscopy Supplement 6, 1992 (pages 315-330) 0892-953X/92$5.00+.00
Scanning Microscopy International, Chicago (AMF O'Hare), IL 60666 USA

AUTOMATIC ORIENTATION ANALYSIS OF MICROFABRIC

N.K. Tovey*, P. Smart[1], M.W. Hounslow and J.P. Desty

School of Environmental Sciences, University of East Anglia, Norwich NR4 7TJ, U.K.
[1]Department of Civil Engineering, University of Glasgow, Glasgow G12 8QQ, U.K.

Abstract

The orientation of features in digitized scanning electron micrographs may be estimated using a technique which examines the changes in intensity in two orthogonal directions about each pixel. Typically, over 250, 000 estimates of orientation may be made generating an output image where the pixel value relates to the orientation direction of the feature at the corresponding pixel in the original image. At the same time, a rosette histogram may be generated to give a visual impression of any preferred alignment. These data may be reduced to two parameters specifying the direction and degree of orientation.

A new algorithm involving the passage of a large radius modal filter over the orientation-coded, image examines for clustering of features into domains of similar alignment. Results from the use of different filter radii will be discussed. The resulting domain-segmented image may then be processed using traditional particle feature image analysis routines to determine the size and shape etc. of the domains. Finally, the domain-segmented image may be combined with the original to produce a domain-mapped image, highlighting the various domains in different colour.

The steps outlined above may be run sequentially on each image, and batch processing of a large number of images is possible providing an automatic and objective method of measuring microfabric within images.

Key Words: Microfabric orientation, particulate materials, fabric quantification, back-scattered scanning electron microscopy (SEM), intensity gradient analysis, domain segmentation, consistency ratio mapping, domain mapping, batch processing.

*Address for correspondence:
N. K. Tovey
School of Environmental Sciences,
University of East Anglia,
Norwich
NR4 7TJ, U.K.

Telephone: 44 (0)603 56161
FAX No: 44 (0)603 501179

Introduction

The microfabric of a particulate material may be defined as the spatial arrangement of the constituent particles and the associated voids. At a larger scale, such as that visible to the naked eye, the fabric of a soil or sediment may be considered as the geometrical arrangements of aggregates of particles in the form of *peds* and the associated voids and cracks within the material. It has long been recognised that both the fabric and the microfabric have a controlling influence on the physical properties of those materials. Many models have been advanced as to how the fabric deforms under load or the flow of water, and the current situation was recently reviewed by Bennett et al. (1990), where they considered several possible mechanisms of deformation.

In attempting to develop constitutive models to describe the deformations of soils, Engineers frequently make simplifying assumptions regarding isotropy of the material. In more sophisticated models, a degree of anisotropy may be included, but there is a general lack of knowledge as to the extent of these effects and how they relate to the overall mechanical properties, and, in particular, the response to both consolidation (ground settlement) and shearing (such as slope stability). Some hypotheses assume that the particles behave individually, while others postulate that the particles may aggregate into sub-parallel groups or *domains*, and it is the response these domains that controls the overall behaviour. A discussion of these hypotheses may be found in Smart and Tovey (1992). For Geologists and Soil Scientists a study of the microfabric has proved invaluable in understanding the diagenesis of soils and sediments. Besides these hypotheses regarding the response of microfabric to external stressing, the inter-relationships of microfabric with water flow, through the soil, and desiccation and freezing of the soil are of equal importance to Engineers, Geologists, and Soil Scientists. Finally, all branches of Earth Sciences require a knowledge of the diagenetic processes, and for this, microfabric studies are a key part.

Numerous qualitative studies of microfabric have been carried out using all branches of microscopy, but few studies have been quantitative. Some notable exceptions include Lafeber (1967), Morgenstern and Tchalenko (1967a,b) using optical microscopy; Tchalenko et al. (1971) using both optical microscopy and x-ray diffraction; Tovey (1973) using photogrammetry on SEM images; Tovey and Wong (1978) using optical diffraction methods; and Wenk (1985) using x-ray texture studies. The development of image processors, analysers, and powerful image processing and analysis software for use on personal computers now provides the possibility for much increased quantitative work to appraise the various hypotheses.

Early work towards quantification of soil microfabric was done by Foster and Evans (1971) where they obtained transmission electron micrographs of ultra thin sections of embedded kaolin, and used basic image analysis facilities to assess porosity. A similar approach was adopted by Bennett et al. (1977) when studying the fabric of Mississippi Delta clays. More recently, Bisdom and Schoonderbeek (1983) used image analysis to characterise the shape of mineral grains in optical sections of soils, and others have continued work to assess porosity (e.g. Bui and Mermut, 1989). Equally, Ehrlich et al. (1984) have used mathematical morphological methods in defining pore shapes and sizes.

Most analytical techniques for quantifying images of soils rely on the need to threshold the image into a binary or multiple discrete grey-level form to segregate the separate components within the image. This thresholding is not a trivial problem as the general grey level of an image may vary from one part to another, and decisions are needed on whether or not to separate touching particles. While image processing methods may help in this respect, other techniques are needed if objective, automatic methods (i.e. with out operator intervention) are to be developed.

It is apparent that segmentation techniques other than those based on thresholding are more useful for several applications. This paper describes one such method, but other segmentation methods such as those using co-occurrence statistics (e.g. Unser, 1986, Haddon and Boyce, 1990), or fractal dimensions (e.g. Keller et al. 1989), may also prove to be helpful in automatically delineating areas of soil microfabric which have different textural patterns, but these are not yet fully developed. Equally, others such as the "Watershed Segmentation Method" described recently by Beucher (1992) may also warrant attention.

Intensity Gradient Analysis

Unitt (1975) devised a technique to measure orientation using an intensity gradient technique. This algorithm is a form of edge detection for which there are many different types (e.g. Haralick, 1984); however, it is not the detection of edges that is important, but the evaluation of the orientation of intensity gradient vectors. These vectors relate directly to the orientation of features within the image edges. The whole image is scanned, and the vector is determined at each pixel. The direction of each histogram may be classified in a suitable rosette diagram, which, when plotted, will show the nature and direction of any preferred orientation. With this information obtained, it is possible to reduce the results to typically two parameters: one specifying the preferred orientation direction, and the other a measure of the strength of the orientation (an index of anisotropy) which may be related to the bulk properties of the material. An important advantage of the technique is that it relies on intensity changes rather than absolute values, and does not suffer from the problems associated with thresholding and/or segmentation which are a pre-requisite for many other methods.

In 1980, Tovey developed the intensity gradient technique and applied it specifically to the study of soil fabric. In addition, he considered a number of factors which may affect the performance of the method. In particular, he examined two micrographs taken at 90° to one another, and showed that the difference in orientation between the two images as measured by the technique was within 1 degree of 90°.

The method was extended by Tovey and Sokolov (1981), while in 1988, a fully general formulation was derived (Smart and Tovey, 1988). Several more recent papers have used the method, and in particular have highlighted practical aspects:- Tovey et al. (1989, 1990), Smart et al. (1990), Tovey (1990), and Sokolov and O'Brien (1990).

While measures of the preferred orientation direction and also the degree of orientation are important in defining relationships between external stress and microfabric, it is also of importance to study how the particles aggregate and move relative to another. A domain may be defined as a sub-parallel aggregation of particles, and some hypotheses regarding soil deformation suggest that it is these domains which determine the overall macroscopic properties of the soil within the whole fabric (see Bennett et al. 1990). In this paper, a discussion of techniques used to map automatically the shape and size of such domains is given. It is an extension of the work reported by Smart et al. (1990), and is a natural development of the intensity gradient method. Some applications of the technique were considered in Tovey et al. (1992), but this paper considers many of the practical aspects not covered previously.

Methods

The procedures used in the analysis to automatically define and map features of similar orientation are summarized in Fig. 1. There are several steps in the analysis and organised so that batch processing of images is possible.

The analysis may be summarized as follows, and begins with image acquisition, followed by an intensity gradient analysis which generates a new image which codes the orientation at each pixel. This new image may then be used for display purposes, or statistical analysis to derive key parameters defining the degree of orientation. A form of cluster analysis to examine groupings of pixels may be done to define areas with similar general orientation. This process, known as *domain-segmentation* (also referred to as *top-contouring* by Smart et al. 1990) produces a further image in which the grey level values at each pixel indicates the class to which that pixel belongs. This last image is in a convenient form for assessing sizes and shapes of the domains, and also for combination with the original image to generate a colour-coded, domain-mapped image.

Image Acquisition

Samples of soil were impregnated with Araldite AY18 resin, and the resulting blocks ground and polished to give a flat surface suitable for observation in the back-scattered mode of operation of a Hitachi S450 SEM. A typical image is shown in Fig. 2, and from the same series as used by Hounslow and Tovey (1992) for other analysis procedures. In the image, the higher atomic number kaolin particles generally appear brighter than the darker embedding medium. The particles are all elongate, and one purpose of the quantification techniques under development is to assess the extent of alignment of these particles. The sample had been previously consolidated to a stress of 700 kPa in the vertical direction and then deformed in triaxial shear. In this image, there is little evidence of the previous vertical stressing (which would be manifest by a dominance of horizontally orientated particles).

The SEM was carefully calibrated using two precision grids so that precise data regarding the size of pixels at each magnification was available. The grids were observed at several different magnifications, and on digital images of these grids the distances between bars were measured several times. A calibration curve was thus computed enabling the effective pixel size to be extracted at any given magnification. This calibration is repeated at regular intervals in the authors' laboratory.

Digital images were acquired using a LINK Analytical interface with a single pass over the image taking some 20 seconds. A careful calibration of the SEM was made to ensure that all images were acquired at approximately the same dynamic range. One way to do this is to set a given level for the particles, and a second level for the voids. However, this is not feasible for this type of sample for several reasons. Firstly, even though nearly pure kaolin was

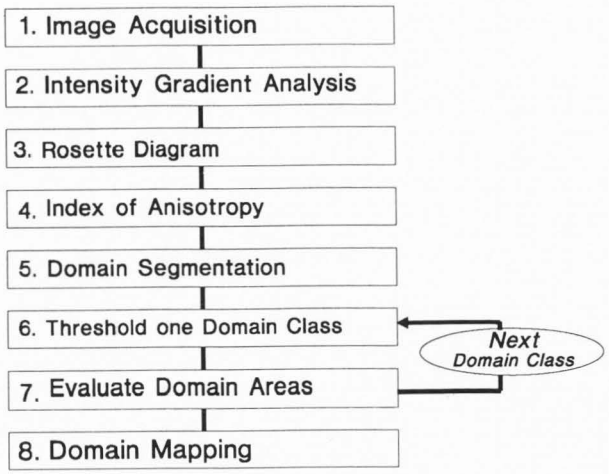

Fig. 1. Flow chart showing steps in automatic orientation analysis.

used, the composition does vary with some particles, rich in iron, appearing brighter than other particles. Secondly, several particles are submerged just below the surface and thus do not contribute fully to the 'particle' signal. Thirdly, even at high magnification, there are rarely areas of sufficient size of either the voids or the particles to ensure proper calibration. Accordingly, a polished, resin-impregnated specimen of quartz grains was used. In this both the particles and the resin are large and of uniform composition. It was found that setting the grey-level to 230 on a quartz particle, and 40 in a void provided images with the full dynamic range with little problem for saturation.

The selection of the correct magnification for observation is an important factor in any analysis. Thus the pixel spacing must be chosen so that at least one pixel falls inside the smallest feature (i.e. voids or particle) that is likely to be of interest. In the observation of the soil fabrics used as examples in this work, the individual clay particles are typically 0.3 - 0.5 μm thick while the voids are sometimes a little smaller. In the SEM - image acquisition currently available, the pixel spacing at 2000 x magnification was 0.110 μm, and this was generally consistent with the features present. The choice of spacing seems sensible, but this matter will be discussed further when results from the intensity gradient analysis are considered.

Intensity Gradient Analysis

The orientation of features within an image is assessed using the intensity gradient technique, recent developments of which may be found in Smart and Tovey (1988) and Tovey et al. (1989). In this analysis method, the change in intensity in two orthogonal directions at each pixel location is computed. Unlike many edge operators which use only the pixels immediately adjoining the pixel in question, the algorithms developed above use different groupings of pixels in the 5 x 5 (or larger) array surrounding the pixel. In its most simple form, only the changes in intensity from the pixel in question to that immediately above, and that immediately to the right, are considered. In such situations the intensity gradients in both the x- and y- directions (i.e. dI/dx and dI/dy) are computed. A more general approach was described by Smart and Tovey (1988), and the following summarizes the key points.

In a more general sense, the intensity I_n at the n^{th} point in a 5 x 5 pixel array may be expressed by a two dimensional expansion of Taylor's theorem:-

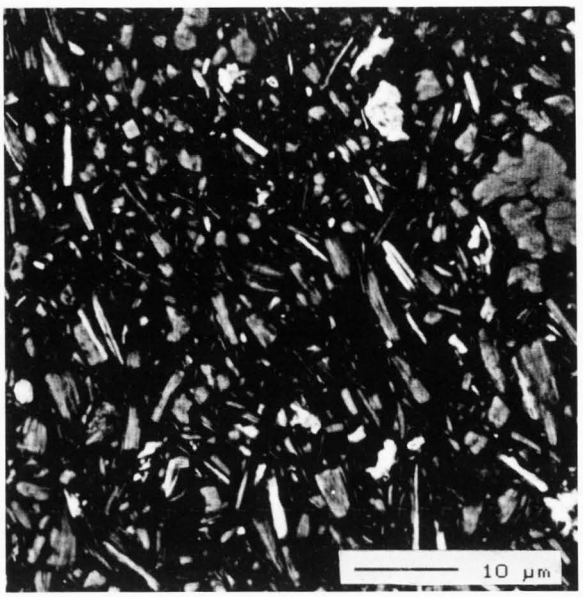

Fig. 2. Typical back-scattered electron SEM image of a polished surface of consolidated kaolin embedded in resin. The image was digitised using a Link Analytical AN10000 interface with a pixel resolution of 512 x 512 and a grey level resolution of 0 - 255.

$$I_n = I_o \cdot \exp(h_x D_x) \cdot \exp(h_y D_y) \qquad (1)$$

where $D_x = \frac{d}{dx}$ and $D_y = \frac{d}{dy}$

The full expansion of equation (1) gives two terms of the first order, three terms of the second order, four of the third order etc, for example the four coefficients of the third order terms are:

$$\tfrac{1}{6}h_x^3 D_x^3 + \tfrac{1}{3}h_x^2 h_y D_x^2 D_y + \tfrac{1}{3}h_x h_y^2 D_x D_y^2 + \tfrac{1}{6}h_y^3 D_y^3$$

While only the first order terms are needed to specify the intensity gradient vector, all other terms from higher orders must be eliminated by using intensity information from sufficient points. Thus 2, 5, 9, 14, and 20 data points are required for solution to a 1st, 2nd, 3rd, 4th, and 5th order respectively. Normally, it is desirable to have more than the minimum number of points when least squares adjustment becomes possible. Using this approach a matrix containing 24 rows (number of surrounding pixels) and 20 columns (sufficient for a fifth order solution) may be constructed, and any sub-set of this matrix may be used to specify the formula for a particular grouping of pixels.

Of particular relevance to the current study is the circular grouping of 20 pixels (i.e. excluding the corner pixels in the 5 x 5 array) in a fourth order solution. The coefficients for dI/dx as a function of the intensities at the surrounding pixels may then be computed as:

	0.013	0	-0.013	
0.077	-0.207	0	0.207	-0.077
-0.070	-0.280	0	0.280	0.070
0.077	-0.207	0	0.207	-0.077
	0.013	0	-0.013	

while a similar but orthogonal set of coefficients is relevant for dI/dy. Other sets of coefficients are relevant for the 1st, 2nd, 3rd and 5th order solutions.

The above arrangement of pixels was used throughout the current study, while Tovey and Martinez (1991) have shown that a second order formulation based on the 8 nearest pixels gives almost identical values for orientation as the above fourth order solution, and also saves up to one third in computing time. However, in other applications (for instance the domain segmentation described below), they found this lower order method not as suitable.

Two minor difficulties arise in the computation. Firstly, it is not possible to compute orientation vectors within 2 pixels of an edge with the current formulation. There is no reason why asymmetric formulae should not be used, but, for simplicity, these have not been used in the current study, and consequently the computed angles-coded images will be 508 x 508 pixels in size instead of the normal 512 x 512. Secondly, in regions of the image where there is little or no contrast, the evaluation of the orientation vector can become indeterminate as it has low or zero magnitude. Typically this is of little consequence as such areas rarely cover more than 1% of an image, and normally cover less than 0.1%. Tovey (1980) and Tovey and Smart (1986) outline criteria for dealing with such areas.

Results obtained from Intensity Gradient Analysis

Three separate sets of information may be derived during intensity gradient analysis. Firstly, a new image in which the intensity is a direction function of the evaluated orientation at each pixel may be generated. This is known as an angles-coded image in which the orientation values, to the nearest degree, are recorded in the range 0 - 180. Any pixel at which the orientation is indeterminate is coded to 255. Secondly, a further new image may be constructed showing the magnitude of the intensity gradient vector at each point, and thirdly, a histogram may be constructed to show the frequency distribution of angles of a given orientation. In this histogram construction, class widths of 5° are normally used, but other class widths may be used provided that criteria for dealing with vectors of low magnitude are adjusted accordingly (see Tovey, 1980, and Tovey and Smart, 1986 for more information on this matter).

The angles-coded image following intensity gradient analysis of Fig. 2 is shown in Fig. 3. It is a little difficult to visualize the full effect in monochrome, and normally a special colour look-up table is generated to highlight the different orientations. The orientation convention used here is for angles to be measured clockwise from the upward vertical (following the compass bearing convention in Earth Sciences) rather than the normal mathematical convention. Dark regions in Fig. 3 are close to the upward vertical whereas lighter areas are nearly 180° clockwise to this direction. The bright areas correspond to areas in which the orientation is indeterminate. Generally, Fig. 3 is difficult to interpret visually, but may be used as the starting point for the domain segmentation discussed later.

It is helpful to reduce the data from the 250,000 estimates of orientation into just two parameters, one giving the direction of any preferred orientation, and the second giving the strength, or degree, of that orientation. Several methods exist for generating these parameters. One convenient method is the presentation of an unweighted rosette such as the one shown in Fig. 4. Alternatively, one of two methods involving some form of weighting may be used. In the first, the frequency is weighted according to some function of the magnitude of the intensity gradient vector. Though this may be of value in some circumstances, decisions as to the exact form of the weighting function are needed. In the unweighted form, the advantage remains that the histogram distribution is affected little by changes in mean intensity and contrast in the original image. Examples of both weighted and unweighted rosette diagrams were given by Tovey et al. (1989). In the second method, separate histograms are constructed for different ranges in the magnitude image, and this was used to advantage by Tovey and Krinsley (1990) to highlight two distinct directions of preferred orientation.

Normally unweighted histograms are generated, and in most situations the form of the rosette diagram approximates to an ellipse. It is a simple matter to derive the equation of the best fitting ellipse to this distribution, and from that to define an index of anisotropy based on a ratio of the lengths of the major and minor principal axes. A discussion of various indices based on these ratios is given in Tovey et al. (1989), while a more general discussion covering other situations was given in Tovey et al. (1992). When non elliptical distributions are present, one method to proceed involves the computation of the orientation and magnitude of the resultant vector **R**:

In two dimensions,

$$\mathbf{R} = \sqrt{(\sum r_i \cos\Theta_i)^2 + (\sum r_i \sin\Theta_i)^2} \qquad (2)$$

where r_i is the magnitude of the ith vector and Θ_i is the direction of this vector. Reiche (1938) and Smart and Tovey (1982) use an alternative formulation by using the components, x_i and y_i, of the ith vector parallel to the x- and y- axes respectively:

$$\mathbf{R} = \sqrt{(\sum x_i)^2 + (\sum y_i)^2} \qquad (3)$$

This magnitude may be normalized by dividing by the sum of magnitudes of the vectors to give **R'**:

$$\mathbf{R'} = \frac{\mathbf{R}}{\sum r_i} \qquad (4)$$

The direction of this normalized vector specifies the preferred orientation direction and is given by:

$$\Theta_i = \text{atan}\,(\sum y_i / \sum x_i) \qquad (5)$$

The value of **R'** may be used to assess strength of orientation as described by Rock (1988). The normalized resultant vector **R'** has also been called the *Consistency Ratio* (**C**) which was first mentioned by Reiche (1938), and also described by Smart and Tovey (1982). Like the index of anisotropy, **R'** or **C** also range from zero for a random fabric to unity for a perfectly aligned one. In most situations unweighted vectors are used, and in these cases the denominator in equation (3) equals the total number of particles.

For most applications, however, an index of anisotropy (I_a) defined as:

$$I_a = 1 - \frac{min}{max} \qquad (6)$$

is convenient. Here the quantities *min* and *max* refer to the lengths of the minimum and maximum principal axes of the ellipse defined by the least squares fit to the rosette diagram. In the example shown in Fig. 4, I_a is 0.380.

It is to be expected that in particulate materials the index actually measured will depend on the magnification.

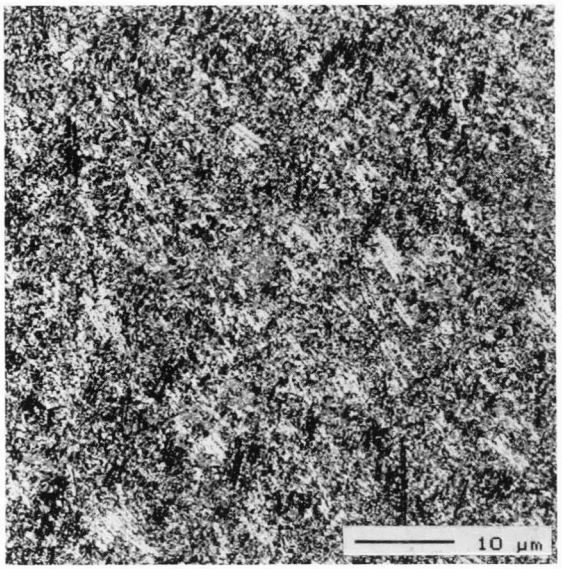

Fig. 3. Angles-coded image derived from Fig. 2. The pixels are coded so that all pixels with the same orientation are the same shade of grey. Generally, darker regions refer to features with near vertical orientation while the shade becomes lighter as the orientation angle increases (clockwise).

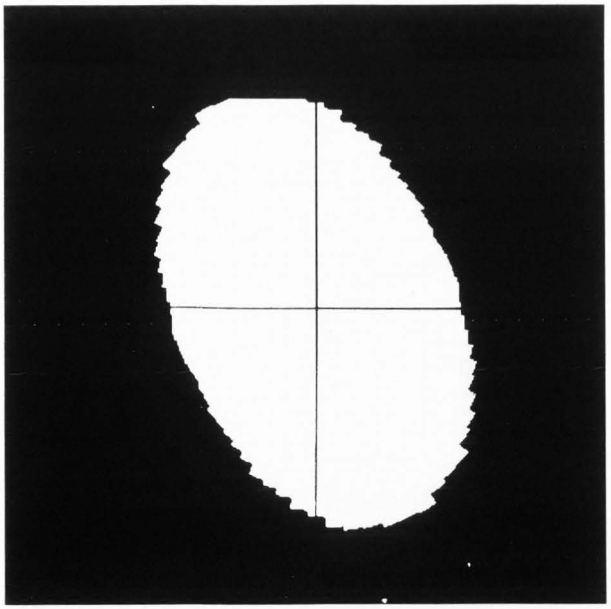

Fig. 4. Rosette orientation diagram showing distribution of pixels with given orientation. The diagram was constructed from over 250,000 separate estimates of orientation and clearly shows the preferred orientation direction. The anisotropy of the sample may be judged from the shape of the distribution: in this example $I_a = 0.380$.

At high magnifications the area covered may have only one dominant domain, but with several smaller ones. In such cases, the index of anisotropy will be relatively high, being close to that in the dominant domain. On the other hand, as the magnification is decreased, areas with other dominant orientations are likely to be included, and this will have the effect of reducing the value of I_a.

Effects of Magnification/Pixel Spacing

Tovey and Sokolov (1981) analysed a few of micrographs using the intensity gradient technique. The micrographs formed a concentric series of magnifications, and negatives of these were digitized at a number of different aperture sizes. Thus an image at 1000x digitized with an aperture of 50µm produced an image approximately 500 x 500 pixels. Equally, an image at 500x digitized with an aperture of 25µm gave an identical pixel resolution for the area common to both images. Both images gave almost identical results when analysed. If, on the other hand, the area common to both images was digitized with a 50um aperture in the x500 image, then the index of anisotropy was found to be lower than for the higher magnification image. Finally, if the higher magnification image was digitally reduced, then this was found to also reduce the index by the same amount. From this it is thus clear that the effective pixel resolution is important, but it does not matter whether this has been achieved by direction digitization or by subsequent digital reduction.

As a more detailed investigation 24 separate SEM images spaced at 2mm across a sample of embedded kaolin were acquired at 2000 times magnification, and intensity gradient analyses used to estimate indices of anisotropy. While there was some consistency in the values measured, there were clearly regions of the sample where the fabric was less ordered than in other areas. From these images a further series of images was generated, and for each series the magnification was reduced by 10%, i.e. the magnifications used were: x2000, x1800, x1600, x1400 ..... x200. In this way it was ensured that exactly the same area of each image was covered at each of the ten magnifications.

For the ten series of images, each series taken at a different magnification, both the index of anisotropy and orientation were evaluated by the intensity gradient technique, and both parameters were then plotted against magnification as shown by examples in Fig. 5. There are two points to note from the diagrams. Firstly, the orientation directions appear to have erratic values up to approximately x500, and thereafter, the orientation in each image remains approximately constant. Secondly, there are notable variations in the index of anisotropy with magnification. This is to be expected as, when the pixel resolution is insufficient, it will not be possible to discriminate between separate particles. For all 24 images, there was a gradual decline in the value of the index as the magnification was reduced from x2000 to approximately x1000 as noted by Tovey and Sokolov (1981), but thereafter, substantial changes took place. In some images, the index fell off linearly but steeply below this magnification, while in others, the index showed an erratic trend as the magnification was reduced.

In the earlier work of Tovey and Sokolov (1981), a consistent decline to x500 was noted. However, in their case they were using a coarser grained material and would need to extend their observations to x100 or lower to detect the effects noted here. It would appear that at approximately x1000 the individual particles are indeed being resolved and that there are only slight changes with increasing magnification. Below this magnification, only aggregates are resolved, and these will initially tend to be more equi-dimensional (i.e.

lower index), but as the magnification further reduces these aggregates may themselves be associated with others giving a more aligned appearance, and hence the variation noted in some images in the low magnification region. It would appear that the initial choice of x2000 magnification for the bulk of the research reported in this paper, and which is near the resolution of high quality images, was a sound one. There is little variation in index for small variations in this magnification. It would also appear that there is a fundamental difference in the spatial arrangements of particles and aggregates at a size just resolved at x1000, i.e. about 0.22μm.

Domain-Segmentation

The angles-coded image (Fig. 3) derived from intensity gradient analysis shows the orientation at each pixel, but it is usually very difficult, even to the trained eye, and even with the aid of colour. In some classes of images, linear features at near constant orientation will stand out clearly, but in many other cases, the image presents just a mosaic of colour. It is often useful to be able to assess general aggregations within an image rather than the detail of orientation at each pixel, which, by definition, will be much smaller than the majority of features present. A way to proceed is to pass a filter over the angles-coded image to examine for clusters of pixels depicting features lying in the same general direction. This process is known as *Domain-Segmentation* (also referred to as *top-contouring* by Smart et al. 1990). Two methods have been used. The first, more approximate, but faster method, was briefly described in Tovey et al. (1992). The second is more mathematically robust, but needs up to over four times the computing time as the approximate method on PC type machines.

In this second method a large radius filter is centred on each pixel in turn over the angles-coded image. The angle of orientation of the intensity gradient vector at each pixel is first doubled, and a resultant vector mean direction computed from the vectorial sum of all the pixels within the masked region. Finally, the direction of the resultant vector is halved, and the central pixel value replaced by the direction corresponding to the resultant vector. The doubling and halving procedure is needed to avoid the difficulties arising as to which of the two directions (at 180° to one another) should be chosen to specify the rod-like (or plate-shaped) particles (Curray, 1956; Rock, 1988). Normally, it is helpful for future interpretation to actually code the central pixel to a particular histogram class. For purposes of presentation in this paper, it may be assumed that just four classes are used for the histogram; i.e. vertical, horizontal, and two directions inclined at 45°. Thus if the mean resultant vector direction was computed in this situation to lie within ±22.5° of vertical it would be assigned to class 1 representing pixels with a general vertical orientation. Similarly, other classes may be defined as follows (noting that 0° is vertical, and all directions are measured clockwise from the upwards vertical):

1 - vertical (i.e within ±22.5° of vertical)
2 - bottom left to top right (i.e. from +22.5° to +67.5°)
3 - horizontal (i.e. from +67.5° to +112.5°)
4 - top left to bottom right (i.e. from +112.5° to +157.5°)

For more detailed work, 8, 12, 16, or 18 (corresponding to 10° class widths) may be used, but, for simplicity of presentation, the four class method will continue to be used in this paper.

During the computation of the normalized mean resultant vector for the area within the mask, its magnitude $\mathbf{R}'$ is also evaluated, and this can be used as the basis of the Rayleigh Statistical test to check whether or not the area differs from random at the 95% or other defined level (see Rock, 1988). If the value is significantly different from random, then it is coded to the histogram class determined, otherwise it is coded as a fifth ("random") class. The mask is passed over the whole image, and the resulting *domain-segmented* image will consist of pixel values only in the range 1 - 5 in this example with four basic orientation classes.

The *domain-segmented* image will be reduced in areal coverage by the radius of this mask at each image boundary, unless separate coding algorithms are constructed for using asymmetric masks. This was not done in this particular research. Essentially, *domain-segmentation* creates an image which separates the image into a limited number of regions of generally consistent orientation. An example, using 4 orientation classes (+ one "random" class) is shown as Fig. 6. Fig. 6b is the *domain-segmented* image of Fig. 6a. In this example, only the outlines of the domains are shown. An alternative method of presentation is to show all the domains having a particular orientation coded as a particular grey level (Fig. 7a). Here the darkest areas refer to vertical domains with the brightest corresponding with the "random" areas. Further improvements in presentation are gained if this figure is masked with one to highlight the directions of the separate domains (Fig. 7b). The "random" areas in this image are shown by series of dots.

The size of the mask chosen could have a profound effect on the form of the segmentation. Thus a domain of particles which is much smaller than the diameter of the mask will be lost in the background of the larger surrounding domain. Fig. 8 shows the effect of changing the radius on the total number of domains detected using the resultant vector method to avoid any interactive effects. The number of domains detected declines exponentially, but begins to level out at a pixel radius of 15-20. The same effect is illustrated in the images shown in Fig. 9 which are the central region of Fig. 2. In Fig. 9b (radius 7), there are many more domains than in Fig. 9e (radius 39 pixels), and at the same time the area covered by "random" regions decreases. Careful examination of the images shows that these "random" areas generally coincide with voids and the edges of small domains.

In Fig. 9e it is apparent that several small horizontal domains are lost within the large inclined domain (e.g. the horizontal domain near the centre of Fig. 9a). On the other hand, many of the domains present in Fig. 9b are small, often no larger than a particle, and thus by definition can hardly be called domains. An optimum radius lies between these two extremes, and the value of 19 chosen for this research is reasonable. For other particle sizes, and/or magnifications, other radii should be chosen.

While the resultant vector method may be used, the approximate method (mentioned by Tovey et al. 1992) executes nearly 4.5 times faster in the PC MS-DOS environment, and thus has advantages when speed is of importance. The speed of execution depends both on the radius of mask used, and on the type of computer. In Table 1, the times taken for typical *domain-segmentations* on a 512 x 512 byte image are compared for two machines. It can be seen that the Rayleigh method for *domain-segmentation* takes over 1250 seconds on the Dell for a radius of 19 pixels. This time is unacceptably long, and it was for this reason that the more approximate method was developed. The time now drops to 289 seconds. On the SUN IPC Sparcstation, the difference in timing is much less noticeable, and for the full Rayleigh method, just 45 seconds is needed for the same task. Table 1 also shows the effects of varying the radius of the Mask.

Clearly if only a PC environment is available, it is important to consider the alternative, approximate algorithms described by Tovey et al. (1992). In this method, the angles-coded image is first transformed so that the angular values are replaced by the class values as indicated above. Essentially, the method replaces the central pixel by the modal value

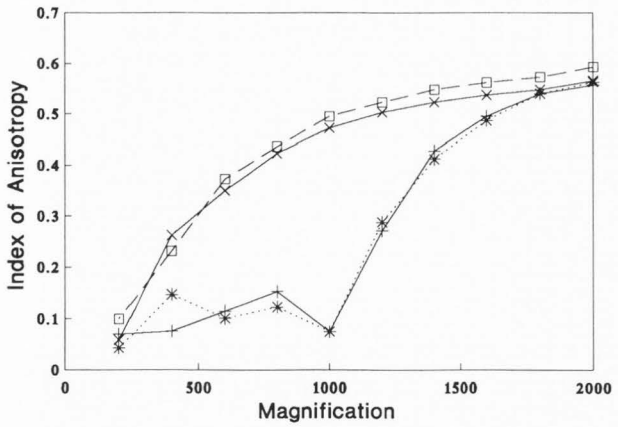

Fig. 5. Variation in index of anisotropy with magnification for 4 separate areas of a sample of embedded kaolin particles. At x2000 magnification (corresponding with an effective pixel resolution of 0.110 μm), there are only slight changes in the index with changes in magnification. At lower magnifications the choice of magnification is critical.

TABLE 1. Effects of radius of mask and computer type on execution time.

radius (pixels)	DELL 80286 (20Mhz) timings (secs)		SUN IPC Sparc Station 1 timings (secs)	
	Rayleigh	Approximate	Rayleigh	Approximate
3	-	-	16.3	-
5	-	-	17.7	-
7	-	-	21.9	-
11	-	-	30.5	-
19	1258	289	45.1	28.3
29	-	-	60.1	-
39	-	-	72.9	-

subject to certain criteria. Fig. 10 shows a typical situation with a mask having a radius 6 pixels. Here the dominant class is "4", and the central pixel is thus replaced by this value. In situations where there is no dominant class, a value of "5" random is coded to this pixel, but some simple criterion is needed to determine this situation. This criterion is likely to vary both with radius and with the number of classes chosen. In the four class case, the percentage (T) of the dominant class must exceed 25%, and accordingly was formulated as:

$$T = \frac{(100 + exc)}{400} \times 100 \qquad (7)$$

where T is the percentage which must be exceeded, and "*exc*" is a variable, the value of which may be chosen to any value between -100 and 300. This formulation gives a convenient way by which to compare the approximate method with the more formal method, and thereby select the optimum value of "exc" which should be used.

Fig. 11 shows the results derived from six very different images. The ordinate indicates the area of the domains segmented as random, while the abscissa indicates the value of "exc". As might be expected, all curves appear to increase exponentially. The value of "exc" which generated a random

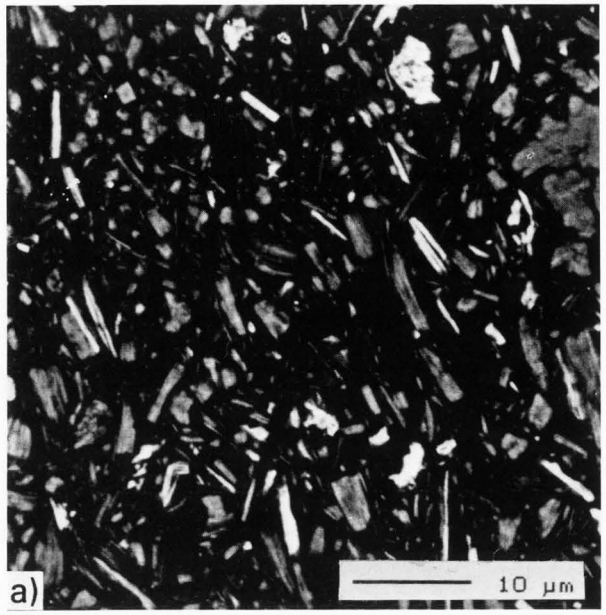

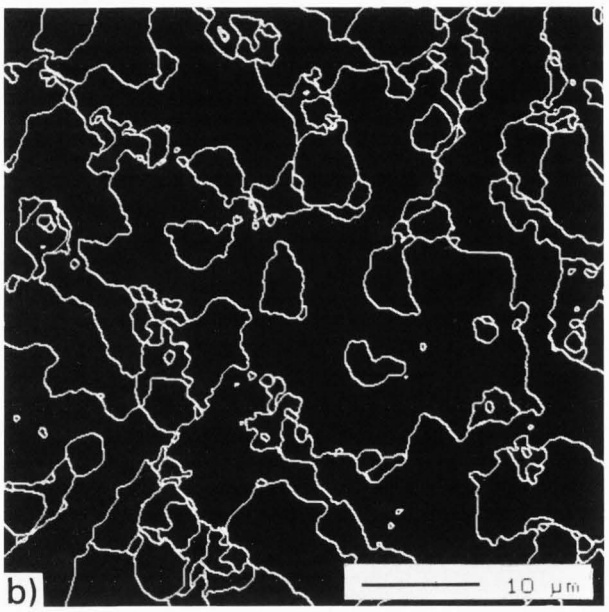

Fig. 6. An example of *domain-segmentation* using a mask of 19 pixels radius and the Rayleigh method for ascribing classes. In this example, four primary orientation directions were used plus one class to denote "random" areas. The separate "regions" are outlined in Fig. 6b which can be overlaid on the original (Fig. 6a) - see also Fig. 13.

domain area most consistent with the full statistical method was noted and is marked on Fig. 11. In all cases, the optimum value of "exc" for a radius of 19 appears to be close to 10, and accordingly this value is now used in analysis. If either the number of domain classes, or the statistical level is changed from 95%, then clearly the value of "exc" must be changed as well. Fig. 12 illustrates the same effect on one image where the value of "exc" is varied. When this value is large (_100), almost the whole image is classified as random, while if exc is zero, no random areas are present. Table 2

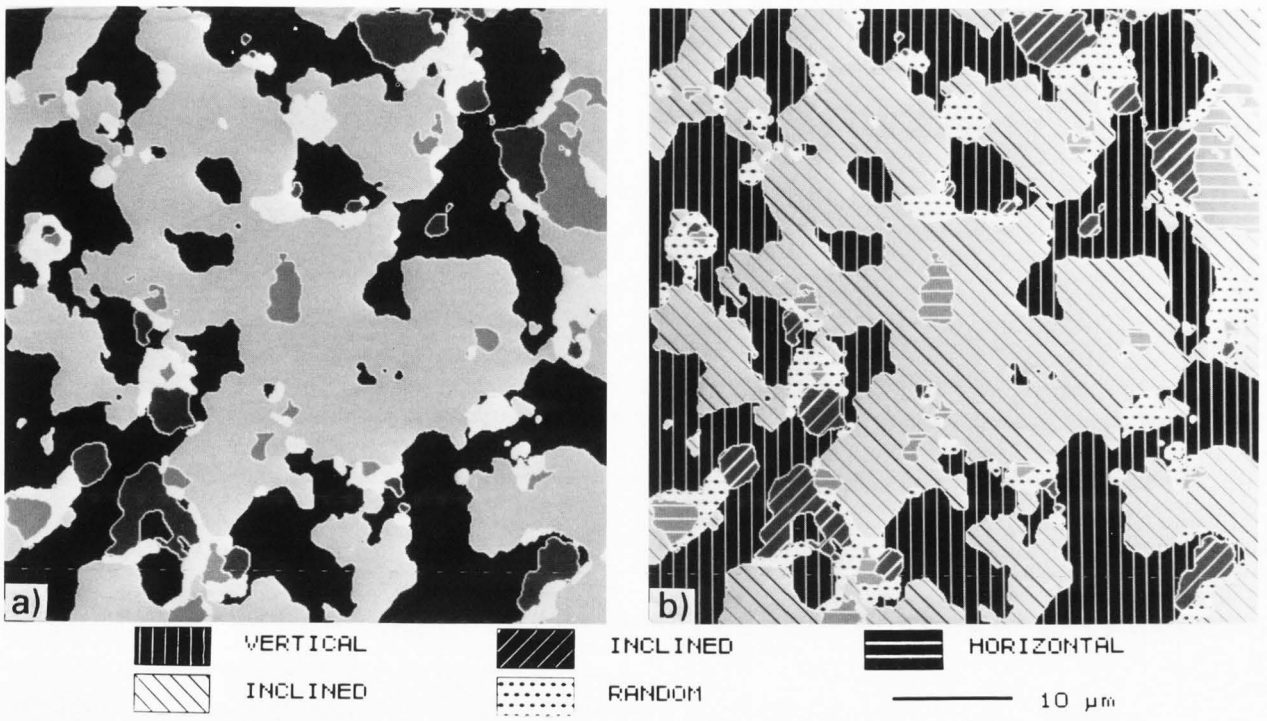

Fig. 7. Alternative method for presenting *domain-segmented* images. Fig. 7a shows the separate domains coded to a different grey-scale value. Fig. 7b overlays Fig. 7a with a series of patterns to highlight the general directions. The original image is shown in Fig. 6a for comparison.

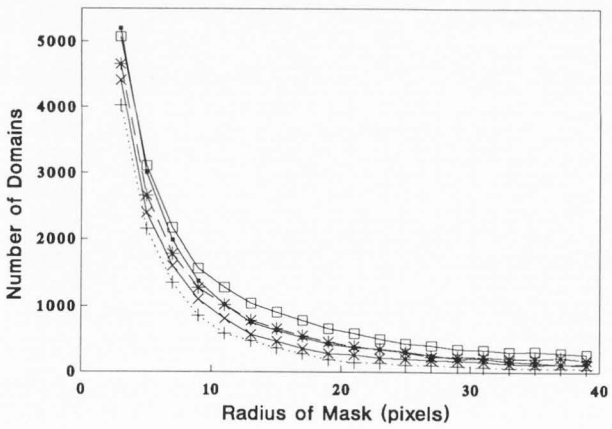

Fig. 8. Variation in number of domains segmented with the radius of the mask. The number falls rapidly at first and then declines little after about 15 - 20 pixel radius.

indicates the optimum values of "exc" which generate a *domain-segmented* image which bears close resemblance to that generated by the resultant vector method for several different radii. The figures were derived by analysing several very different fabrics, and in all cases, the optimum values were within ± 1 of the values shown.

Domain-Size Analysis

Once an image has been segmented in a manner described above, it is a simple matter to select just one group of domains and generate a binary image at a particular grey-scale value which shows these domains alone (step 6 of Fig. 1). The percentage area of the image covered by that class may then be computed (step 7 of Fig. 1), and then repeating the binary image transformation, but this time at a different grey-scale level, enables the areas of the other sectors be evaluated.

TABLE 2. Variation of optimum value of "exc" with radius of mask. The values of "exc" above produce a *domain-segmented* image using the faster approximate method which is very similar to the mean resultant method.

Radius	Optimum value of exc
7	28
11	17
19	10
29	6
39	4

Thus in Figs. 6b and 7, the relevant percentage areas are as follows:

vertical (sector 1)	- 38.7 %
inclined - bottom left/top right (sector 2)	- 5.2 %
horizontal (sector 3)	- 4.1 %
inclined - top left/bottom right (sector 4)	- 44.3 %
randomly orientated domains	- 7.6 %

Once the image has been coded into domain, it is possible to use the routine particle statistic analyses available in most image processors to assess the size, shape, orientation, perimeter, and other parameters about each domain.

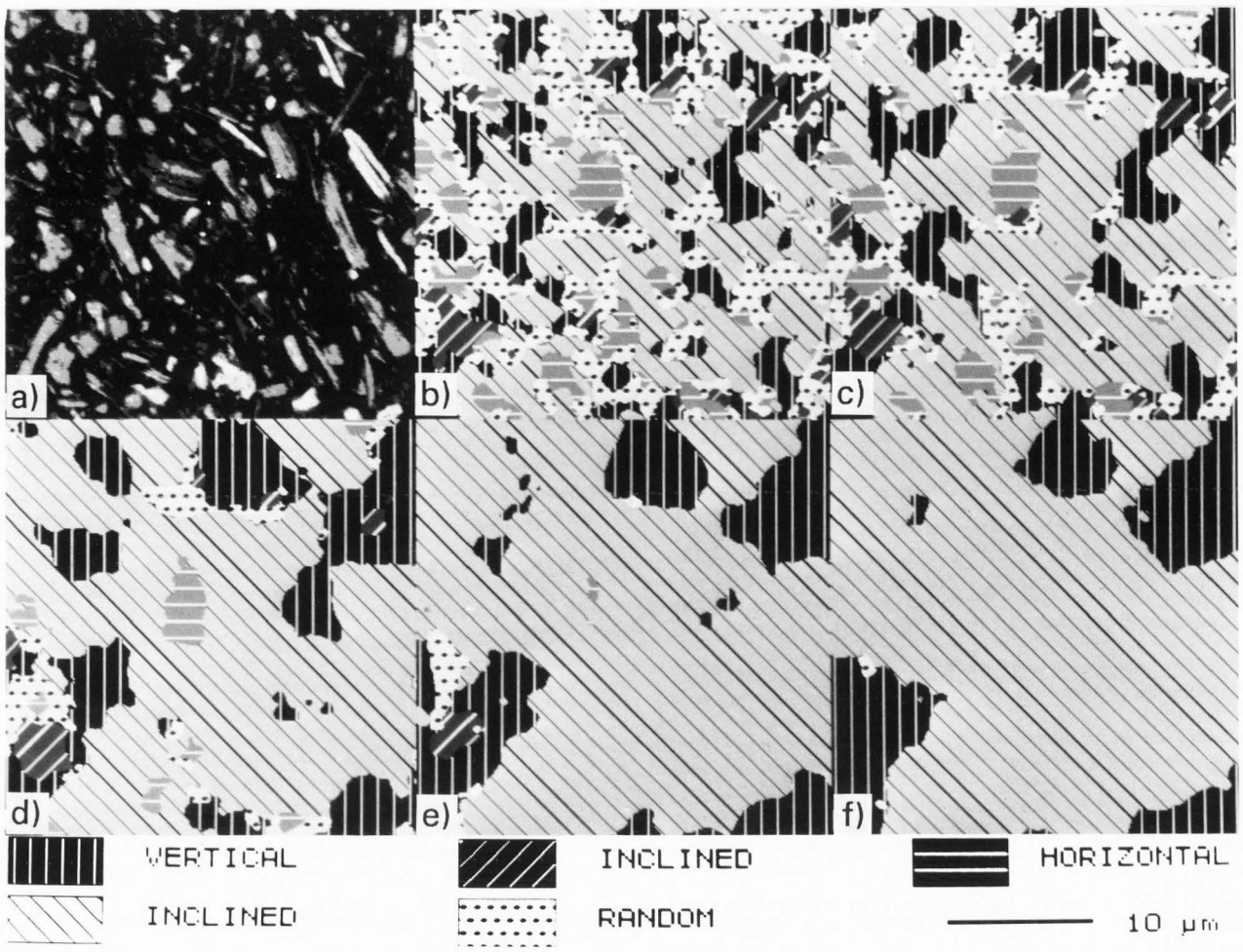

Fig. 9. A pictorial representation of data in Fig. 8 for selec ted radii of the mask for the central portion of Fig. 2: a) original image; b)-e) different radii; b) 7 pixels; c) 11 pixels; d) 19 pixels; e) 29 pixels; 39 pixels. For the larger radii, smaller domains are lost in the dominant orientation; at smaller radii, there are several domains which are hardly larger than a single particle. The optimum size to preserve most domains appears to be around 15-20 pixels.

Thus, in theory, it should be possible to examine how domains of particles change both in size and orientation, as soils and sediments deform under stress or through the migration of fluids.

Domain Mapping

The *domain-segmentation* described above provides a method to quantitatively assess domain aggregations in particulate materials, however, it is not so easy to visually compare the individual regions with one another. A further step (step 8 in Fig. 1) is therefore required, called *Domain-Mapping*. In this, the boundaries between the different domains obtained in the *domain-segmented* image may be overlaid on the original image. Thus Fig. 13 shows the effect of overlaying the boundaries to the regions in Fig. 6b onto the original image in Fig. 6a. While this figure is of some help it is not easy to appreciate which are classified as one class, and which are classified as another. Presentation in the form shown in Fig. 14, can be helpful as only those domains with a particular orientation are highlighted. Fig. 14a shows just the vertical domains outlined with the remainder masked, while Fig. 14b shows the same effect using an eight orientation class segmentation for comparison. This latter figure clearly shows the advantage of the higher number of orientation classes. A further helpful way of presentation is to apply a colour transformation, so that the original grey-scale image is colour shaded according to the orientation of the domain, and display the image using a specially constructed look-up table. The monochrome equivalent is shown in Fig. 15, but without the aid of colour, the full effect cannot be, but the general texture can still be observed.

Practical Considerations

There are several practical points to consider in the techniques described here.

1) Soil fabric can vary considerably over just short distances, and in most analyses, it will be necessary to study large numbers of images if overall bulk properties are to related to changes in particle packing etc. It is essential that image processing techniques are developed which permit automatic analysis of fabric. There are two ways to aggregate the results from intensity gradient analysis from the different images at a particular magnification. A straight arithmetic mean may be computed, or alternatively, the vector mean value may be computed. Both techniques have their merits. The former is a useful

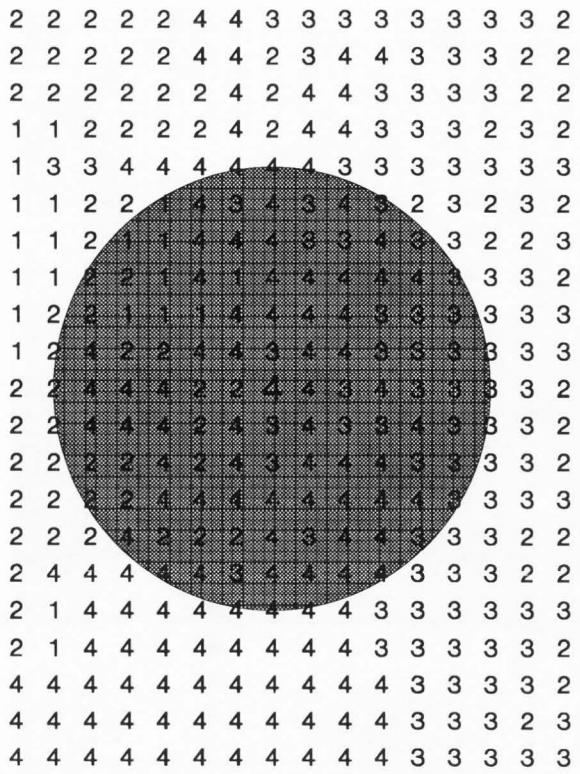

Fig. 10. Illustration of the approximate method for *domain-segmentation*. The example shown here uses a pixel radius of 6.

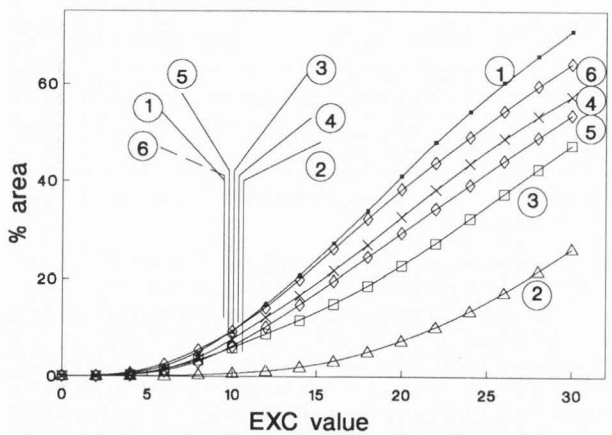

Fig. 11. Variation of the parameter "*exc*" with percentage of "random" regions. This parameter is used as a criterion for assessing "random" regions in the approximate method. Six images with very different fabrics were used in this analysis. For a mask radius of 19 pixels, an "*exc*" value of 10 seems optimum.

way to assess how the average anisotropy of the relatively small areas covered by each image varies. The vector mean method meanwhile gives an indication of the mean value over a larger area, and is more useful when relating the mean anisotropy to external stress level. When the images have a single dominant domain, the two methods give similar mean values. As the fabric becomes more random differences as much as 50% may occur.

2) The number of domains identified in an image is often large > 500-1000, and it is normal practice to store up to 25 parameters such as area, perimeter, orientation, as well as several shape factors, and the storage requirement can create major problems. Whatever radius is used for segmentation, there will always be very small areas defined, and often these are of particle size and thus do not form a domain in the strict sense. It is an easy matter to disregard these in any analysis, and recode the areas as the surrounding major domains. In this analysis, an area covering 40 pixels (i.e. 5 x 10^{-13} m^2, and consistent with that of a whole particle) was taken as the threshold cut-off criterion. Removing such small features reduced the total area analysed by less than 1%, and in most cases less than 0.1%.
3) A related point refers to the small irregularities on the edges of each domain. These, once again, are perturbations of a size smaller than that of a particle, and were removed by smoothing using a 5 x 5 median filter.
4) Several of the domains in any image will touch the edge, and many of the measured parameters, such as shape and orientation etc. become meaningless or irrelevant for such domains. On the other hand, the area covered by such domains is important in assessing the overall proportion of domains of features lying in one direction as opposed to another. Clearly, there must be some method to discriminate between domains touching the edge, and those which do not, so that the domains may be correctly included in whichever parametric analysis is required.
5) It is necessary to consider which parameters are most meaningful for the analysis in hand. There is little difficulty with parameters such as total area, number etc, but parameters such as shape have many different definitions. In the work on soils, it has been the authors' experience that shape defined by a ratio of the second principal moments provides a more robust measure of shape than other definitions including feret diameters etc. Equally, for size measurements, a definition using mean moments is to be preferred over straight area measurement.
6) Most other fabric analysis methods rely on thresholding to generate a binary image, and it is this stage that is frequently the most difficult and which involves operator intervention. The techniques described here rely not on absolute intensities, but on relative intensities, and thereby do not require supervision. The whole procedure from the intensity gradient analysis through to domain mapping can be achieved in a batch mode by repeating the stages in Fig. 1 for groups of images. It is common practice to group 36 or more such images in a single batch run in the author's laboratory. This does require that special management procedures are set up so that the results are output in a compact and convenient manner.
7) Several new algorithms have been developed in this work, and all have been incorporated as extension commands into the SEMPER image processing and analysis package (available from Synoptics Ltd, Cambridge Science Park, Cambridge, UK). This is now permitting batch processing of large numbers of images using the techniques described.

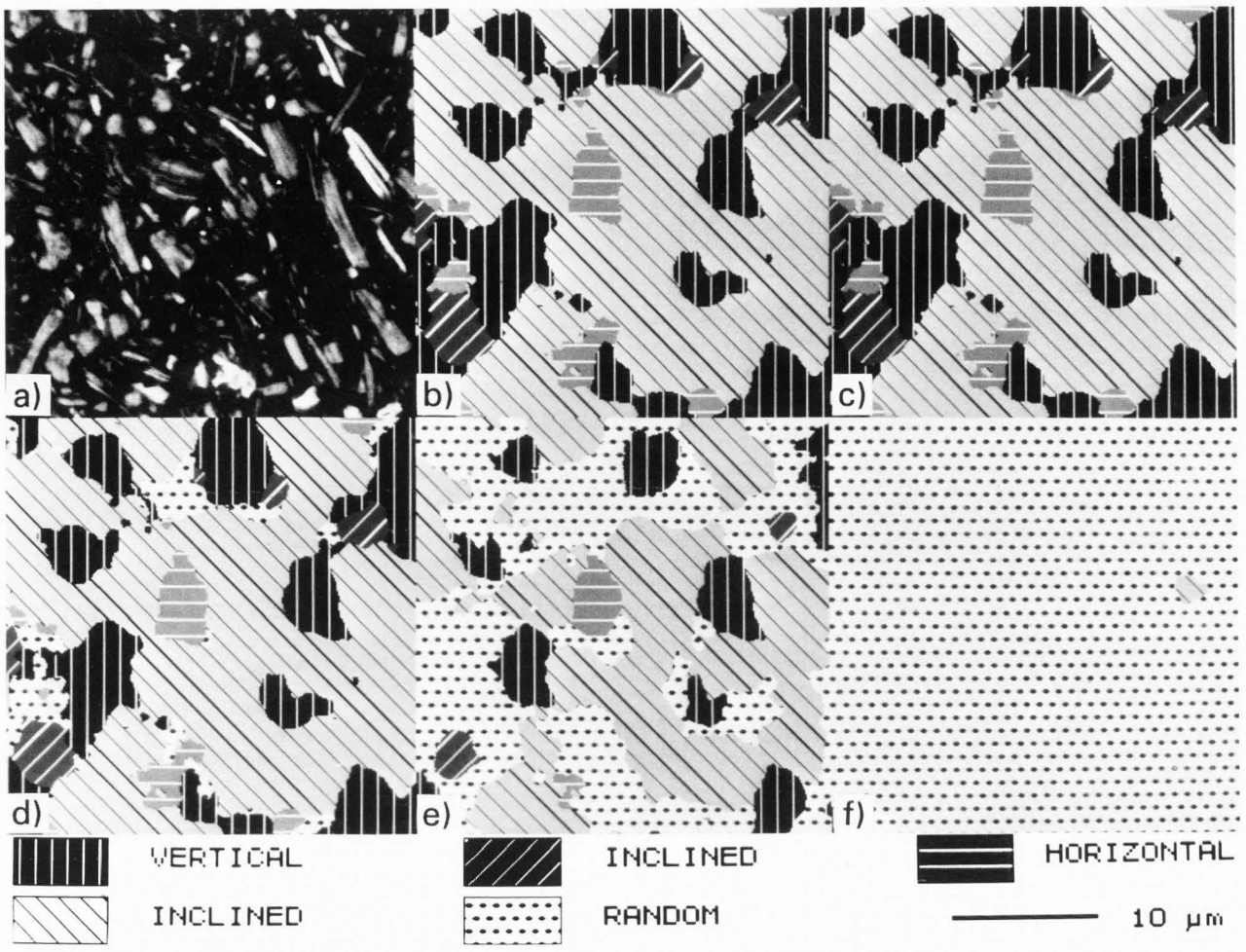

Fig. 12. A pictorial representation of data in Fig. 11. Fig. 11a is the original image (reproduced from Fig. 9a). Figs 11b- 11e show the effect of selecting different values for *exc*: b) *exc* = -100; c) *exc* = 0; d) *exc* = 10; e) *exc* = 25; *exc* = 100. As the value increases, the area coded as "random" increases. Fig. 12d (from the approximate method) closely resembles Fig. 9d which is the equivalent image using the Rayleigh method.

Some Results

The purpose of this paper has been to describe techniques: the bulk of the results obtained during the use of this technique are to be reported elsewhere in Engineering and Geological literature. However, there are some results which it is important to include here in addition to those mentioned in Fig. 5. Fig. 16 shows the average number of domains in each image is strongly correlated (negatively) with the anisotropy index. This is to be expected since an increase in index implies that a higher proportion of features are aligned in the preferred orientation direction leading to fewer but larger domains. Conversely the index of anisotropy shows a strong positive correlation with mean domain size.

Fig. 17 shows the results from two orthogonal traverses across a single sample. A total of 24 separate images were taken (12 on the horizontal traverse, and 12 on the vertical traverse) at a magnification of x2000, and at the standard spacing of 1.0mm. On the vertical traverse, the index of anisotropy varies relatively little from 0.502 to 0.577. On the other hand, the horizontal traverse shows a variation from 0.593 to 0.310, with a change in anisotropy of as much as 0.2 over just 1.0mm. It would seem that though there may be some consistency in anisotropy within the fabric in some regions of a sample on the microscopic scale, there are inhomogeneities at the scale of millimetres. Clearly fabric analysis must be conducted at all levels if a full understanding is to be gained. This is particularly important as the variation within a sample can be as great as variation between samples.

Discussion and Conclusions

Using the techniques described in this paper, it is now possible to automatically map the orientation of features within micrographs of soil fabric to quantitatively assess the degree of orientation, and determine the extent of aggregation. Unlike conventional image processing methods, the intensity gradient technique does not suffer from the normal thresholding problems, and provides results which can be readily aggregated over several images. The choice of magnification and effective pixel resolution is important, and on a 512 x 512 pixel resolution, a magnification of x2000

Fig. 13. *Domain-segmented* image of Fig. 2 generated by overlaying Fig. 6b on Fig. 2.

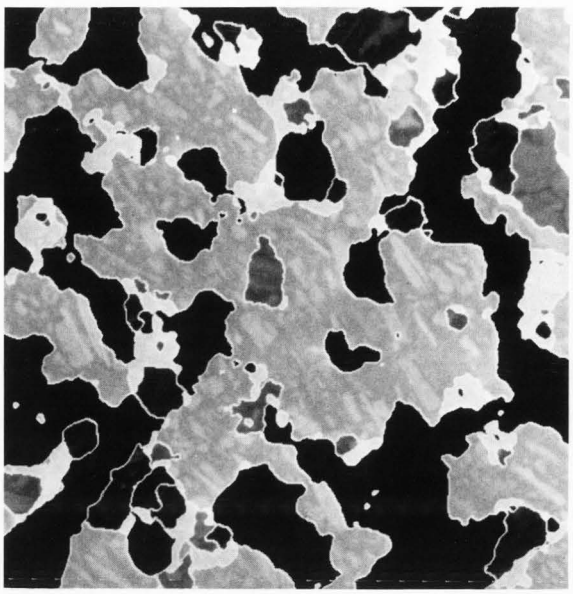

Fig. 15. *Domain-mapped* image of Fig. 2 generated by rescaling image in Fig. 2 and multiplying by image in Fig. 7a. The actual version is best visualized with a specially constructed look-up table. In the author's laboratory, the vertical domains are shown in varying shades of red, while the horizontal ones have a range of blue intensities etc.

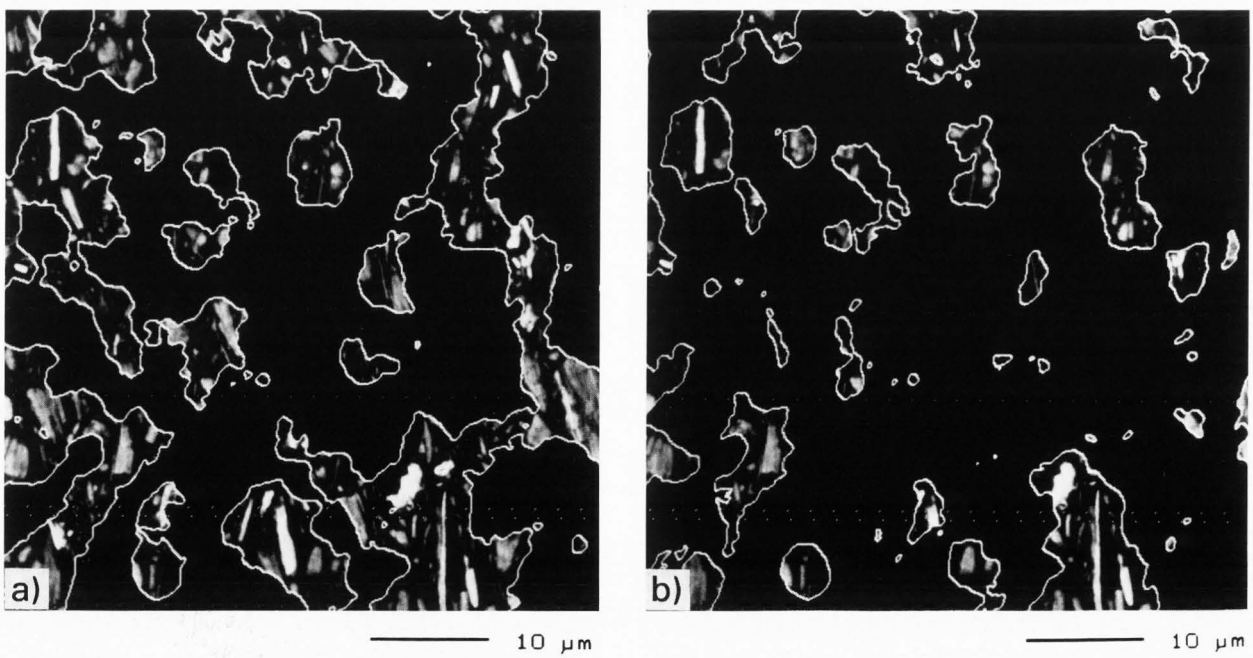

Fig. 14. A further method for presentation of *domain-segmented* images. Here the original grey-scale image is combined with Fig. 6b, but all region except those for the vertical domains have been masked. Fig. 14a shows the situation using four orientation classes; Fig. 14b shows the similar situation if eight orienta tion classes are used.

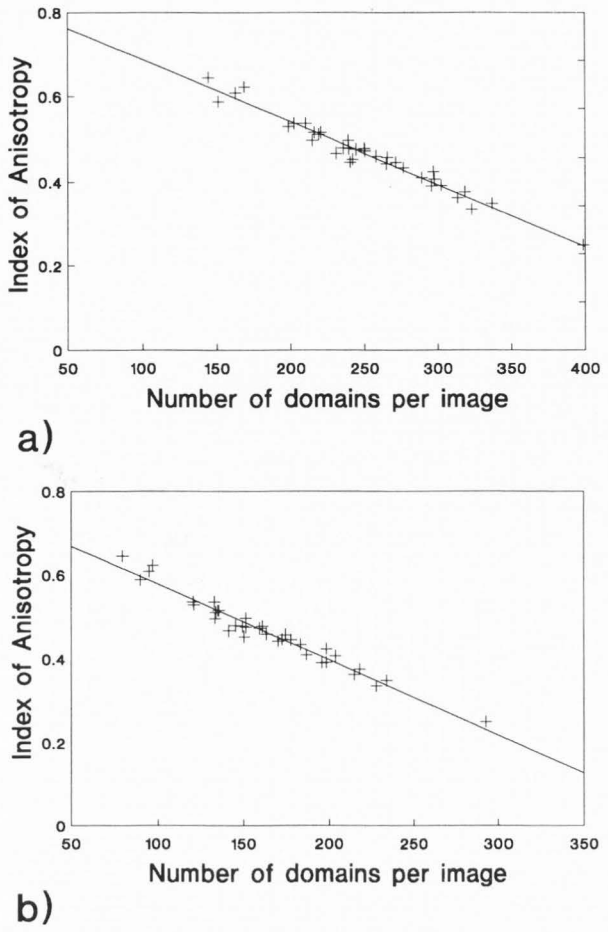

Fig. 16. Variation of index of anisotropy I_a with number of domains. Data presented here was acquired from over 500 images. Fig. 16a: data from segementation using 12 primary orientations; Fig. 16b: data from using 8 segments.

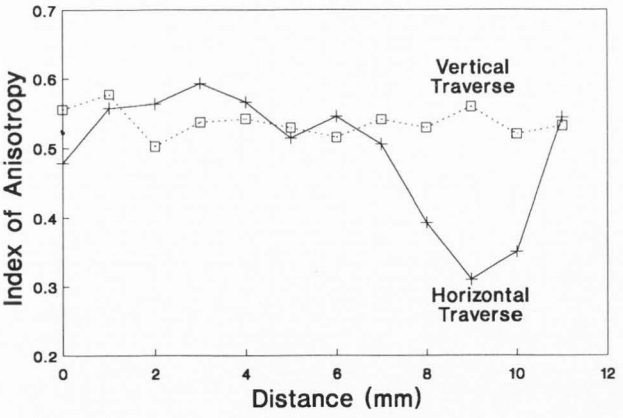

Fig. 17. Variation of the index of anisotropy (I_a) with distance across a sample. While there is often consistency between one image and neighbouring images, there can be marked differences over regions at the scale of millimetres.

gives a pixel spacing of 0.110μm. For kaolin particles, this is a sensible combination as the results vary little with small changes in either of these parameters. With the same material, effective pixel spacings of about 0.2μm or above (i.e. magnifications less than x1200 at 512 x 512 pixel resolution) would seem to be unwise choices.

Two versions of a *domain-segmentation* method have been described. The more general resultant vector method is a better choice, but can take up to 4.5 times as long as the more approximate method on a PC computer. With the approximate method, parameters may be selected which give very close approximations to the resultant vector method for a wide range of fabrics. However, these parameters will vary depending on the number of domain classes chosen, and also the radius of mask.

A *domain-segmentation* method using four orientation classes plus one random class has been described. Two different approaches to the technique were considered. The approximate method has also been referred to as *top-contouring* (Smart et al. 1990), while the more formal method is identical with *consistency ratio mapping*. The number of classes was chosen to aid in the preparation of micrographs for display. For detailed work it is advisable to use a higher number of orientation classes such as 8, 12, 16, or 18. Values above 18 would seem to have little merit, as the final domain segmented images are extremely difficult to understand, and contain vast number of domains, the results from which require a vast storage volumes.

Domain-mapping achieved by combining the *domain-segmented* image with the original provides a convenient method for display and visualization. However, the full effect of this can only been seen in colour.

Finally, none of the several stages in the analysis require operator intervention, and it is possible to group large numbers of images to analyse them successively in a batch mode.

Acknowledgements

The authors wish to acknowledge financial support from the US Air Force Office for Support for Research (AFOSR Grant No. 87-0346). Technical support from Stephen Bennett is also acknowledged.

References

Bennett RH, Bryant WR, and Keller GH, (1977). Clay fabric and geotechnical properties of selected submarine cores from the Mississippi Delta. NOAA Professional Paper 9, U.S. Department of Commerce, 70-82.

Bennett RH, Bennett WR, and Hulbert MH, (1990). Determinants of clay and Shale Microfabric Signatures: Processes and Mechanisms. In: Bennett, R.H. O'Brien, N.R. and Hulbert, M.H., Microstructure of Fine-grained sediments, from mud to shale, Springer-Verlag, New York, 5-33.

Beucher S, (1992). The Watershed transformation applied to Image Segmentation. Scanning Microsc. Supplement 6, 299-314.

Bisdom EBA, and Schoonderbeek D, (1983). The characterisation of the shape of mineral grains in thin sections by Quantimet and BSEI. Geoderma 30, 303-322.

Bui EN and Mermut AR, (1989). Orientation of planar voids in vertisols and soils with vertic properties. Journal Soil Science Society of America. 53, 171-178.

Curray JR, (1956). The analysis of two-dimensional orientation data. J. Geology, 64: 117-131.

Ehrlich R, Crabtree SJ, Kennedy SK, and Cannon RL, (1984). Petrographic image analysis, I. Analysis of Reservoir Pore Complexes. J. Sedimentary Petrology, 54: 1365-1378.

Foster RH and Evans JS, (1971). Image analysis of clay fabric by Quantimet. Microscope 19: 377-401.

Haddon JF and Boyce JF, (1990). Unification of image segmentation and edge detection. Institution of Electrical Engineers: Proceedings, 137: 129-135.

Haralick RM, (1984). Digital step edges from zero crossing of second directional derivatives. Institution of Electrical and Electronic Engineers: Transactions on Pattern Analysis and Machine Intelligence, 8: 118-125.

Hounslow MW and Tovey NK, (1992). Segmentation of Pores in Back-scattered Images of Sediments and Soils, and their Relationship to Domain Structure. Scanning Microsc. Supplement 6, 245-254.

Lafeber D, (1967). The optical determination of spatial (three-dimensional) orientation of platy clay minerals in soil thin sections. Geoderma, 1: 359-369.

Keller JM, Chen S, and Crownover RM, (1989). Texture description and segmentation through fractal geometry. Computer Vision, Graphics, and Image Processing, 45: 150-166.

Morgenstern NR and Tchalenko JS, (1967a). The optical determination of preferred orientation in clays and its application to the study of microstructure in consolidated kaolin I. Proc. Royal Society, Series A., 350: 218-234.

Morgenstern NR and Tchalenko JS, (1967b). The optical determination of preferred orientation in clays and its application to the study of microstructure in consolidated kaolin II. Proc. Royal Society, Series A., 350: 235-250.

Reiche P, (1938). An analysis of cross-lamination:- The Coconino Sandstone. Journal of Geology, 46: 905-932.

Rock NMS, (1988). Numerical Geology. In: S. Bhattacharji, Freidman, G.M., H.J. Neugebauer, and A. Seilacher (editors), Lecture Notes in Earth Sciences, Springer-Verlag, 18, chapter 6.

Smart P and Tovey NK, (1982). Electron microscopy of soil and sediments: Techniques. Oxford University Press, Oxford, 174-175.

Smart P and Tovey NK, (1988). Theoretical aspects of intensity gradient analysis. Scanning, 10: 115-121.

Smart P, Tovey NK, McConnochie I, Hounslow MW, and Leng XL, (1990). Automatic analysis of electron microstructure of cohesive sediments. In:R.H. Bennett, W.R. Bryant, and M.H. Hulbert (Editors), Microstructure of Fine-Grained Sediments from Mud to Shale, Springer-Verlag, New York, 359-366.

Smart P and Tovey NK, (1992). Microfabric of the Deformation of Soils. In: J. Gill (editor) Proceedings of Particulate Mechanics Workshop, Alberquerque, Air Force Office of Scientific Research, Kirtland AFB, New Mexico, 16-19.

Sokolov VN and O'Brien NR, (1990). A fabric classification of argillaceous rocks, sediments, and soils. Applied Clay Science, 5, 353-366.

Tchalenko JS, Burnett AD, and Hung JJ, (1971). The correspondence between optical and x-ray measurements of particle orientation in clays. Clay Minerals, 9: 47-70.

Tovey NK, (1973). A general photogrammetric technique for the analysis of scanning electron micrographs. In: W.C. Nixon (Editor),Proceedings of Conference on Scanning Electron Microscopy: Systems and Applications. Institute of Physics, London, 82-87.

Tovey NK, (1980). A digital computer technique for orientation analysis of micrographs of soil fabric. Journal of Microscopy, 120: 303-315.

Tovey NK and Wong KY, (1978). Optical techniques for analysing scanning electron micrographs. Scanning Electron Microsc. 1978;1: 381-392.

Tovey NK and Sokolov VN, (1981). Quantitative SEM methods for soil fabric analysis. In: O. Johari (Editor), Scanning Electron Microsc. 1981;I: 537-554, and 536.

Tovey NK, (1990). The Microfabric of some Hong Kong marine soils. In : R. Bennett, W. Bryant, and M. Hulbert (Editors), Microstructure of Fine-Grained Sediments: From Mud to Shale, Springer-Verlag, New York, 519-530.

Tovey NK and Smart P, (1986). Intensity gradient techniques for orientation analysis of electron micrographs. Scanning, 8: 75-90.

Tovey NK, Smart P, Hounslow MW, and Leng XL, (1989). Practical aspects of automatic orientation analysis of micrographs. Scanning Microsc. 3: 771-784.

Tovey NK, Smart P, and Hounslow MW, (1990). Quantitative orientation analysis of soil microfabric. In: L.A. Douglas (Editor), Soil Micro-morphology: A Basic and Applied Science, Elsevier, pp. 631-639.

Tovey NK and Krinsley DH, (1990). A technique for quantitatively assessing orientation patterns in sand grain microtextures. Bull. International Association of Engineering Geologists. 41: 117-127.

Tovey NK and Martinez MD, (1991). A comparison of different formulae for orientation analysis of electron micrographs. Scanning, 13: 289-298.

Tovey NK, Smart P, Hounslow MW, and Leng XL, (1992). Automatic domain mapping of certain types of soil fabric. Geoderma. 53: 179-200.

Unitt BM, (1975). A digital computer technique for revealing directional information in images. J. Physics Series E, 8: 423-425.

Unser M, (1986). Sum and difference histograms for texture classification. Institution of Electrical and Electronic Engineers: Transactions on Pattern Analysis and Machine Intelligence, PAMI-8: 118-125.

Wenk HR, (1985). Preferred Orientation in Deformed Materials and Rocks: An Introduction to Modern Texture Analysis. Academic Press, London, 203-210.

Discussion with Reviewers

G. Bonifazi An extensive discussion about gradient analysis is reported in the paper. Have the authors performed, and then compared, with particular reference to the case of microfabric, the gradient analysis proposed with the "classical ones" such as those based on Roberts, Sobel, Prewitt, and Frei Cheng operators?

Authors: We have investigated both the Roberts and Sobel operators and generally found these to be more prone to noise than the more general formulations we now use. In general we have found that derivative solutions to a high order are generally preferable except where noise is present when a low order solution, but with high least squares redundancy, is preferred. We have not done a comparison with the Frei Cheng operator.

D. Jeulin: It is not clear if the proposed approach is the most appropriate for the example shown as an illustration: the specimen is a set of elongated clay particles out of a dark background. Therefore the orientation information is contained in the orientation of the objects. Despite the fact that the grey level of each particle is not uniform, it seems easy to extract the objects by use of a thresholded gradient or of a morphological top-hat transformation. From the binary image of the objects, we could obtain useful information, such as a global coefficient of anisotropy, but also the distribution of the orientations of the objects, or correlations between the orientations of the neighbouring objects, and so on. Working on the grey-level image does not seem to provide an accurate description of the orientation, as seen from the segmented images in the figures. Did the authors try to work on binary images to characterize their material?

Authors: The printed image tends to show a sharper boundary between the particles and voids. The actual

histogram of intensities is unimodal (see for example Hounslow and Tovey,1992). Attempts to threshold the image into a binary form have been done with some success when it is porosity measurements that are the subject of interest. We are not satisfied that such an approach will reliably, and without operator intervention, separate all particles correctly.

There are usually several thousand features in each image, and the space limitations for storage of the results may limit the scope of such analysis, particularly when several tens of images from each sample are analysed to obtain statistically meaningful results. The situation is not helped by increasing the magnification. This reduces the number of particles in each field of view, but the number of images to be analysed increases. The advantage of the approach taken is that two overall objective parameters are obtained which do measure orientation, which require little space to store, and which can be related to overall properties of the soils.

The rosette diagrams always do seem to give a correct indication of overall orientation even when initial subjective assessments suggest otherwise. In the case of the segmented images, it must be remembered that the definition of a *domain* is a collection of sub-parallel particles. This implies that there will be a range of orientations within each domain anyway. Further, the variation in orientation in the segmented images is more a function of the need to reduce the number of domains used for display purposes than a problem with the segmentation. We normally use 12 orientation directions instead of the 4 shown here for clarity, and better segmentation is achieved.

V.N.Sokolov: Can the suggested method be used for estimation of the separate domain form contribution into the total value of anisotropy index?
Authors: Indeed, once the domains have been defined, the orientation and size of each individual one can be assessed. There are several possibilities for further work here both quantifying the orientation of the domains and also comparing the orientation of particles within the domain with that of the domain. However, problems will arise in defining an orientation and hence the effective contribution to anisotropy for those domains which adjoin the edge of the image.

D. Jeulin: You mention the problem of edge effects involved in domain analysis (see point 4 of Practical Considerations). This is problematic for large domains, in the case of an individual analysis. Many measurements provided by Mathematical Morphology (such as size distributions from opening operations) provide an edge correction, and are not sensitive to the presence of large objects connected to the edges.
Authors: We welcome this comment. The purpose of the work undertaken has to been to develop techniques to segment the image and provide basic assessment of domain sizes etc. The next stage will indeed be to follow the suggestion of the reviewer.

J.A.Swift: The display of orientation within an image for visual evaluation is difficult (e.g. as with colour-coded orientation maps mentioned in the paper). You describe an improved display process, but the image remains to some extent confusing. Are there any other approaches you have tried?
Authors: The display of the segmented image for best visual effect is a difficulty. We currently use all the five methods described in Figs. 6b, 7, 13, 14, and 15. Fig. 7a is the most suitable for subsequent analytical work, but neither this nor Fig. 6b is that helpful for a visual effect. We feel that Fig. 7b clearly shows regions mapped in a given orientation, but this does not allow easy comparison with the original image. Fig. 13 does not help to convey which direction is segmented, while Fig. 15 is better. The best method we have found is the colour overlay method of which Fig. 14 is a very poor black and white representation. In colour all the vertical domains show up in varying hues of red, while the horizontal ones have blue shades. A further problem in the presentation is that the visual impact becomes a particular problem when more than about 4 directions are displayed. We normally analyse in 12 sector directions, but have shown only 4 throughout most of the illustrations in this paper.

V.N.Sokolov: What restrictions are there on the application of the intensity gradient method to orientation analysis? To what modes of SEM operation is it applicable? Can it be used for estimation of orientation of primary binary SEM images including only white and black areas such as those having sharp boundaries between pore and particles?
Authors: There are some restrictions to the use of the method. Noisy images tend to give individual pixel estimates of orientation which may be in error, and in general these tend to give lower values for the index of anisotropy. There are ways of dealing with small variations, and alternatively, other formulae can be used which incorporate a degree of filtering (see Smart and Tovey, 1988). For some purposes, images which contain particles which are large and not plate like should be pre-processed using a multi-spectral technique such as that described by Tovey et al (1992) otherwise noise or fine features on particles will tend to confuse the results. An alternative is to generate the magnitude image (i.e a filtered edge defining routine), and then use this as the starting point for analysis. In other situations, it may well be that it is orientation patterns within grains that are the subject of interest. An application of this was shown in Tovey and Krinsley (1990). There is no reason why the method should not be used for modes of operation of the SEM other than the backscattered mode. Indeed the early work in this area (e.g. Tovey, 1980; Tovey and Sokolov, 1981) use secondary electron images.

D. Jeulin: The gradient operator is very sensitive to the presence of noise, which can destroy the information about orientation. You used a median filter to make the contour smooth. Did you study the effect of noise?
Authors: The gradient operator is sensitive to noise. That is why we use a higher order solution with least squares redundancy to the gradient problem than conventional ones such as the Roberts operator. In computing the index of anisotropy, we segregate the gradient vectors according to magnitude, and only those above a certain threshold do we use in the computation of this index. When we are confronted with a particularly noisy image we normally use a lower order solution but with a higher degree of least squares redundancy. The median filter was not used in conjunction with the intensity gradient operation. Instead it was used after the domain segmentation, and its primary use was to remove odd pixels within larger domains. These odd pixels were smaller than a single particle, and cannot be classed as a domain. It is obviously possible to tackle the problem in alternative ways, but this was not done in the current study.

D. Jeulin: Your approach does not require any operator intervention, which is very interesting for batch image processing. However, as shown in the paper, some parameters of the procedure were optimized from many prior experiments: choice of magnification, the size of the radius of the disc for averaging the gradient, the parameter *exc* (which is a threshold to select the local orientation). Could you estimate the amount of work required in this first step of the study for a new type of image? The choice of the magnification and of the radius are very critical, and depends on the spatial frequencies present in the image. Could it be

possible to use information from the images, such as a correlation function or a Fourier analysis, in order to make their proper selection?
Authors: There are indeed several parameters which need to be optimized. However, the parameter *exc* is only relevant if the approximate method is used. With faster computers, the full Rayleigh Method may be used which obviates the need for selecting a parameter here. In the case of magnification, there is no real alternative to studying a range of options as the effective pixel resolution (i.e. a function of magnification and the number of pixels digitized per line of image) required depends on the size of objects to be studied.

In the case of the radius, there are indeed several possibilities using the methods suggested, or using Geostatistical methods, or even using a mean chord length approach on images segmented by the method outlined by Hounslow and Tovey (1992). Ultimately, the first analysis in future work would be the automatic optimizing of several key parameters. The authors do not see an alternative to the selection of optimum magnification except by methods such as that adopted here, or by direct control of the microscope.

G. Bonifazi: After the segmentation techniques and domain identification, accordingly with four or more directions, it is necessary to derive, as clearly evidenced in the paper, a certain set of information on each subdomain characteristic (single particle) constituting the derived areas. The domain presents obviously an irregular shape. What kind of approach and what kind of algorithms have been employed by the authors in order to perform a domain analysis (particle characterisation) in a completely automatic way?
Authors: At present we do not examine each individual particle, although this is planned in future work. Instead we obtain an aggregate measure as an index of anisotropy and a direction as it is these overall parameters which are significant. In the case of domains, i.e. collections of particles, they are indeed irregular in shape, and we use traditional feature statistics to measure areas, perimeters, feret diameters, various shape factors including those derived from combinations of the feret diameters and also ones based on ratios of the second moments of areas. These we compute automatically within stage 7 of the procedure (see Fig. 1). At present we are evaluating the best domain statistics to use for comparison with the macroscopic properties of the soils, and data from these studies will be reported in due course. However, all the parameters are computed automatically and are stored automatically in a database which can be interrogated subsequently for any desired information.

J.A. Swift: The Engineer probably wants a straightforward answer to the question 'is this soil suitable?'. For the methods described in the paper, what are the effort/elapsed time/computing time/cost involved in providing the typical answer.
Authors: The techniques described in this paper are new applications in the field of Geotechnical Engineering, and at present their role is to supplement traditional Site Investigation Methods and to provide parametric information to describe the behaviour of soils. We currently batch process up to 50 images at a time through several stages of analysis. The computing times per image depends on the machine available. As an example, all 8 steps shown in Fig. 1 take about 130 seconds to complete using a 486 (20MHz) machine. With regard to the cost, this has yet to be assessed as it is still in a developmental stage both with regard to software development and hardware availability.

G. Bonifazi: The micro-discontinuities present inside each grain have a great influence in samples such as those described in the paper. From an image processing point of view this fact can be considered as a noise. The aim of the work is to identify mainly the "profile" of each domain constituted by one or more particles having a preferred orientation. How have the authors developed the "tuning" of the procedure? Considering that an increase in the dimension of the mask used to determine gradient generally means that there is an enhancement in the detection of edges in high-noise environments, but a complementary loss of information linked to small regions (in this case, small particle domains). How have the authors evaluated and solved this fact?
Authors: The majority of the particles in the material studied were only a few pixels wide. In samples which contain a wide range in sizes, and particularly those which are approximately equi-dimensional, noise problems within such grains can be a difficulty. In some recent work on real sediments, we have overcome this problem by defining the areas of the large mineral grains using multi-spectral methods (Tovey et al, 1992). Once these areas have been defined we use them as a mask to 'remove' the large problematic grains from the image before attempting analysis as described in this paper.

The mask size used in defining the intensity gradient coefficient is a function of the noise and of the size of the features. It is important to select a formula which is not two sensitive to noise. The magnification must be carefully chosen (Fig. 5). Below 1200x, for the kaolin used, the results are very varied, but above about 1500x the results change little.

With regard to the mask size during the domain segmentation, we used Fig. 8 and similar figures in our decision to choose a particular radius. This was reinforced by comparability with earlier hand-mapping attempts at segmentation (McConnachie, 1974). The radius of the mask is likely to be dependent on the size and nature of the particles present, and, while all the images used in the current study were of the same basic material, it is recognised that for other materials, and equally important, other magnifications, different radii should be used. There are possibilities to define automatically the optimum radius for a given situation using mean-chord-length intercept values on binary versions of the image.

D. Jeulin: Granlund (1980) made use of the gradient over a disc for the purpose of texture segmentation. This reference should be included.
Authors: The authors thank the reviewer for this information. They were unaware of its existence, and cannot at present comment on its relevance to the present paper.

Additional References

Granlund GH, (1980). Description of texture using the general operator approach. IEEE Proceedings of 5th International Conference on Pattern Recognition, 776-779.

McConnachie I, (1974). Fabric changes in consolidated Kaolin. Geotechnique, 24, 207-222.

Tovey NK and Krinsley DH, (1991). Mineralogical mapping of scanning electron micrographs. Sedimentary Geology 75, 109-123.

Tovey NK, Krinsley DH, Dent DL, and Corbett WC, (1992). Techniques to Quantitatively Study the Microfabric of Soils. Geoderma, 53: 217-235.